https://doi.org/10.3311/PPci.16977

Periodica Polytechnica Civil Engineering, 65(1), pp. 309–319, 2021

Microstructural Characterization and Mechanical Properties of Volcanic Tuff (Malatya, Turkey) Used as Building Stone for the Restoring Cultural Heritage

Muslum Murat Maras[1*], Mehmet Metin Kose[2], Tamer Rızaoglu[3]

[1] Department Civil Engineering, Engineering Faculty, Inonu University, 44280, Malatya, Turkey
[2] Department Civil Engineering Engineering and Architectural Faculty, Kahramanmaras Sutcu Imam University, 46050-9, Kahramanmaras, Turkey
[3] Department of Geological Engineering Engineering and Architectural Faculty, Kahramanmaras Sutcu Imam University, 46050-9, Kahramanmaras, Turkey
[*] Corresponding author, e-mail: murat.maras@inonu.edu.tr

Received: 04 August 2020, Accepted: 23 October 2020, Published online: 10 November 2020

Abstract

Old stone buildings constitute a significant percentage of the residential buildings in many countries. These structures are highly vulnerable, and important losses in masonry structures occur even in moderate earthquakes. Therefore, safety evaluations of these structures have gained significant attention in recent years. In this study, the mechanical, physical and microstructural characteristics of tuff samples used in the old buildings were investigated in Battalgazi within the boundaries of Malatya Province during the Seljuk time. The characteristics of the building materials were examined in detail using in-situ and laboratory tests. Because adequate samples could not be obtained from the historical buildings, quarry areas with the same characteristics were identified. First, original building stone (OBS) used in construction was taken from fallen and unusable blocks. Then, the properties of the restoration building stones (RBS) brought from the quarries were investigated. The RBS samples were also examined using in the laboratory, and the mechanical and microstructural properties of the building components were determined. The dynamic and static moduli of elasticity were determined using ultrasonic pulse velocity and uniaxial compression test. The OBS and RBS samples yielded similar results after the microstructural analyses. Our results showed that the dynamic elastic modulus value was higher than the static elastic modulus value. The results revealed by both methods showed that the static and dynamic elastic moduli were closely linked. The OBS and RBS samples exhibited microlitic porphyritic and vesicular textures and nearly the same mineralogical and textural characteristics.

Keywords

old stone buildings, microstructural characterization, tuff, quarries, elasticity

1 Introduction

Old stone houses in the historical centers of the world have been often ignored without any conservation [1]. Therefore, these buildings are at risk of collapsing after natural disasters such as earthquakes [2]. The masonry buildings are very brittle and have low resistance to earthquake effects [3]. A wide variety of intervention techniques have been used to repair and strengthen these structures that have suffered damage [4]. Before beginning any remediation, it is necessary to analyze the structure and determine the causes of the damage [5]. Two methodologies for stability building include non-destructive testing (NDT) and minor-destructive testing (MDT). While NDT methods do not damage the structure, MDT methods cause slight harm to masonry structures [6]. The properties of the structures that can be detected using these methods is large and includes basic parameters such as bulk density, elastic modulus and Poisson's ratio [7].

Many researchers (Török and Přikryl [8], Apostolopoulou et al. [9]) have used NDT methods to study heritage structures. At the present time, the most widely used NDT methods include ultrasonic pulse velocity (UPV) and the rebound hammer test [10]. These methods yield a better understanding of constructions by providing an accurate diagnosis of their stability [11]. The UPV method has been suggested to be a suitable tool for predicting the dynamic elastic modulus properties of construction

Cite this article as: Maras, M. M., Kose, M. M., Rızaoglu, T. "Microstructural Characterization and Mechanical Properties of Volcanic Tuff (Malatya, Turkey) Used as Building Stone for the Restoring Cultural Heritage", Periodica Polytechnica Civil Engineering, 65(1), pp. 309–319, 2021. https://doi.org/10.3311/PPci.16977

materials. Furthermore, the static modulus of elasticity of construction materials has been measured by the MDT method [12]. Słota-Valim [13] noted that these building materials differences between dynamic and static elastic parameters. Many studies Alexander and Thorton [14], Aggelakopoulou et al. [15] have focused on the relationship between static and dynamic elastic parameters (including Young's modulus and Poisson's ratio). In most cases, these methods have been used to accelerate the standard control for both old and new structures. These different methods shed light on their compositional and structural characteristics [16].

Lubelli et al. [17] have studied these tuffs for historic structures. Heap et al. [18] have widely been researched in zeolitized volcanic tuffs the influence of water on the strength. Germinario and Török [19] have stated that as microporosity of volcanic tuffs used for building and restoration decreases, its durability increases.

Doehne et al. [20] have studied microanalysis of rhyolite tuff stone on to characterize the stone samples. As a result, significant differences were observed in the type, quantity and homogeneity of the distribution of rhyolitic stones, which were examined as microstructural features.

In this study, the microstructural properties of original building stone (OBS) and restoration building stones (RBS) used in the heritage buildings were investigated in Battalgazi within the boundaries of Malatya Province. Historical buildings constructed with tuff stone for restoration purposes in Battalgazi town nearby Malatya-Turkey were demonstrated in Fig. 1. Mineralogical properties of the volcanic tuff stone also were investigated. The microstructural characteristics of the building materials were examined in detail using in-situ and laboratory tests. Non-destructive testing and MDT techniques were used as analysis techniques to detect the mechanical or dimensional properties of the structural elements. The OBS and RBS samples exhibited nearly the same mineralogical and textural characteristics. In addition, these methods were used to determine meaningful relationships between the dynamic and static moduli of elasticity. Consequently, generally, the value of the static modulus of elasticity decreased with decreasing strain ratio.

2 Materials and methods

2.1 Material

Volcanic tuff used as building stone was used in the restoring cultural heritage. The stone has been used for restoration purposes in Turkey in many historical masonry structures due to its variety of colors and its easy processing in Fig. 1. We investigated the microstructural, mechanical and physical properties of the tuff used in historical buildings constructed at Battalgazi within the boundaries of Turkey Province during the Seljuk time about 12th century. Because adequate samples could not be obtained from the historical buildings, Malatya quarry areas with the same characteristics were identified. Original building

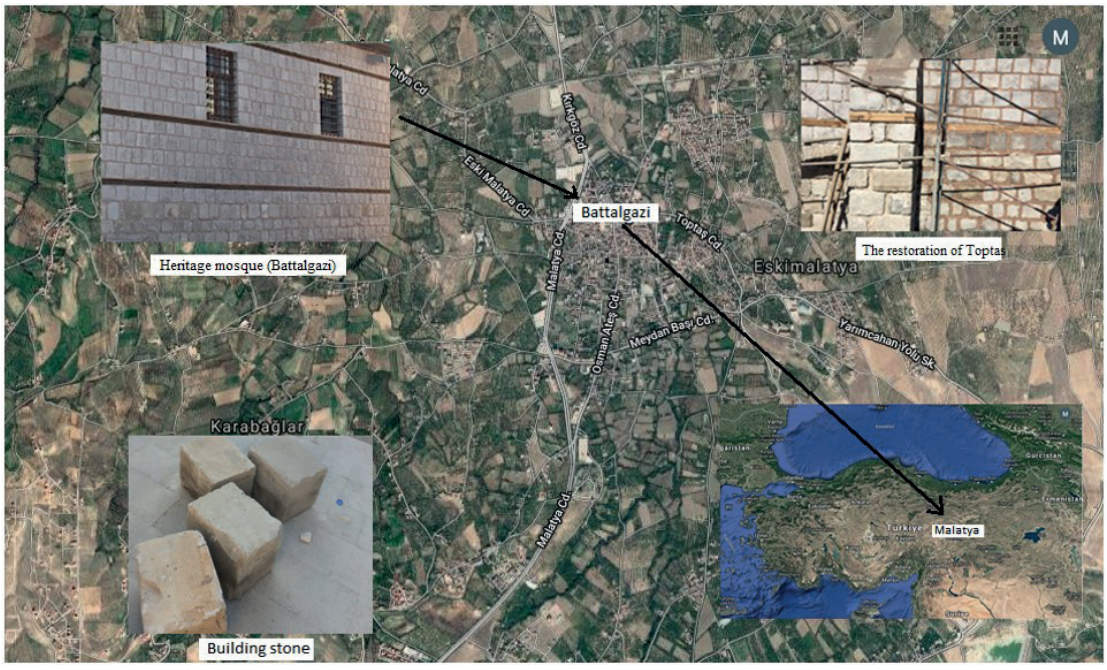

Fig. 1 Historical buildings constructed with tuff in Battalgazi town nearby Malatya-Turkey

stone (OBS) used in the construction was collected from the fallen and unusable blocks, and restoration building stones (RBSs) were brought from the quarry. Volcanic rocks were obtained from quarry to the west of the provincial borders. The stones used in the restoration were removed from the quarry as rocks and then appropriate sizes used as cut stones in 20 cm × 25 cm × 50 cm.

2.2 Methods

2.2.1 Petrographic and geochemical investigations

The microstructure of tuff as a building stone was determined by microstructural analyses. We performed Optical Microscopy (OM) and Scanning Electron Microscopy (SEM) analyses and determined the microstructure properties of the materials used in the structure. Tuff building stone was also analyzed for major and trace elements using X-ray fluorescence (XRF) in the laboratory of Earth Sciences Applications and Research Center (YEBIM) of Ankara University, Turkey. OBS and RBS block samples were analyzed using XRF. The major and trace element contents were determined on glass beads fused from ignited powders to which $Li_2B_4O_7$ was added in a ratio 1:5 in a gold-platinum crucible at 1150°C. The final thin sections were examined using a camera 50i POL model transmitted light at the Department of Geology in Kahramanmaras Sutcu Imam University to determine their petrographical characteristics. In addition, the results of the SEM-EDS analysis using a polarization microscope carried out at IBTAM (Inonu University Central Laboratory, Turkey) were consistent with the reported composition of the raw material. The analyses enabled better three-dimensional observations of the materials. The images of the samples were obtained by scanning the surface with a focused beam of electrons.

2.2.2 In-situ testing

The properties of the building stones were determined using UPV and rebound hardness test method measurements in different locations using NDT methods in the historic buildings. We measured the dynamic modulus of elasticity of the structure using the UPV method. The propagation velocity of compression (V_p) and shear (V_s) pulses was performed in accordance with the ASTM D 2845-05 [21]. The velocities were measured using an ultrasonic instrument (Pundit Lab; Proceq Company). The formation of the signal spreading-receiving instrument was used to measure both the initial ultrasonic transducer couple P-wave velocity and the ultrasonic transducer S-wave velocity. P- and S- wave signals shed light on the damage suffered by structures. In the field of structural conservation, this method can yield data on the dynamic modulus of elasticity of construction materials. We made use of relationships linking longitudinal (P) and shear (S) wave velocities (V_p and V_s, respectively), with density (ρ), the dynamic modulus of elasticity (E_{dyn}) and Poisson's ratio (v).

The relevant expressions are provided below:

$$V_p = \sqrt{\frac{E_{\text{dyn}}(1-v)}{\rho(1+v)(1-2v)}}, \tag{1}$$

$$V_s = \sqrt{\frac{E_{\text{dyn}}}{2\rho(1+v)}}. \tag{2}$$

We used the rebound hammer test, an NDT method to determine the uniformity of structural elements, with the aim of carrying out urgently needed, in-situ tests of old structures. The rebound test hammer housing was applied vertically to the test surface of the building stones. According to ASTM D 5873-14 [22], a total of 20 values were read per sample, and the average value of the surface hardness was calculated the largest 10 readings were taken into consideration. Regression analysis was also performed to determine the overall correspondence between UPV and the surface hardness test.

2.2.3 Laboratory tests

The mechanical properties of tuff are quite important for restoration projects. Tensile and compression tests are used to determine the mechanical properties of the stones used in buildings. Indirect and direct tensile tests can be conducted in a mechanics laboratory. In practice, direct testing is rarely performed because of the difficulties in preparing the specimens. An indirect tensile test is much easier than a direct tensile test in terms of sample preparation [23]; indirect tensile tests have been officially used by the International Society for Rock Mechanics for determining the tensile strength of rock materials (ISRM) [24]. In addition, the compressive strength of a cylindrical sample can be determined with a uniaxial compressive test. The height to diameter (h/d) ratio of samples for such a test is still a matter of discussion. ISRM suggests the use of samples with an h/d ratio between 2.0 and 2.5; Eurocode 7 [25] recommends the use of stone samples with an h/d ratio between 2.0 and 3.0. Samples should be cylindrical with a diameter of preferably not less than NX core size (i.e., approximately 54 mm).

Uniaxial compression test

An experimental study, based on mechanical test, was carried out on chosen representative specimens of the tuff as a building stone used in restoration. The purpose of this assessment was to investigate the mechanical properties of the construction stone. The uniaxial compressive strength (UCS) of the RBS samples was determined in laboratory conditions. Test samples were prepared as cylinders with a height-to-diameter ratio of 2.0–2.5 for the uniaxial compression test according to ISRM (International Society for Rock Mechanics) and a diameter preferably not smaller than the NX (54 mm) core dimension. Three rock samples were carried out in each group for uniaxial compression tests, and the average value was calculated. The core sample is shown under uniaxial compression test in Fig. 2. Linear variable differential transformers were placed on the samples to test their static modulus of elasticity and Poisson's ratio during the compression test.

The compression test of the sample was determined by dividing the ultimate load capacity by the cross-sectional area:

$$\sigma = \frac{P_k}{A}, \tag{3}$$

where σ is the compressive strength (MPa), P_k is the ultimate load (N) and A is area (mm^2).

The static modulus of the elasticity is the slope of the line joining any point of the stress-strain curve to the coordinate center. The secant modulus is called the static elastic modulus because the samples are experimentally determined from the stress-strain relationship. According to Hooke's Law, the load and deflection of a cylindrical elastic layer under the compression test have the relationship shown in Eq. (4). Here, the subscripts θ, r and z indicate the axes along the lateral, radial and axial directions of the sample, respectively. The load-deformation curve of the solid material was detected using a uniaxial compression test in the elastic phase. Poisson's ratio, v and static elastic modulus, E, can be derived from the curves.

$$\sigma_z = -E.\varepsilon_z,$$
$$\sigma_z = \frac{-E.\varepsilon_\theta}{v} = \frac{-E.\varepsilon_r}{v}, \tag{4}$$

where θ, r and z; lateral, radial and axial directions, respectively, σ is the compressive strength (MPa), v is Poisson's ratio and E is static elastic modulus (GPa).

Splitting tensile strength

ISRM suggests using the STS test to measure the tensile strength of building stone. This test is a well-known indirect method in engineering. In this indirect testing method, the specimen is compressed by applied loads and the STS is determined. The results of the tensile strength

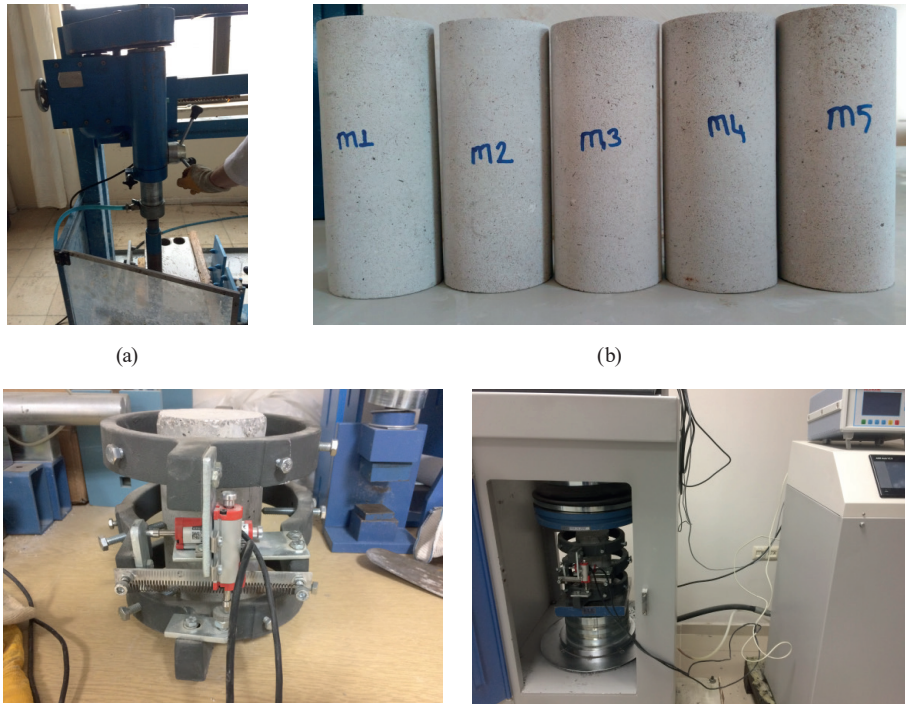

Fig. 2 Uniaxial compression testing setup, a) Core drilling machine, b) Core samples, c) Preparation compression sample before test, d) Uniaxial compression test systems

tests are straightforwardly available if a single straight plane of fracture is responsible for the rupture of the specimen. In the case of shear fracture after the test, the results should be neglected to avoid an incorrect determination of the STS test of the construction material [26] Eq. (5) presents the STS, σ (MPa), perpendicular to the forced diameter at the center of the disc at the time of failure when the applied force is F,

$$\sigma = \frac{2F}{\pi Dt}, \tag{5}$$

where F is failure load (N), D is diameter (mm), and t is thickness (mm).

Physical characterization

Different physical parameters of the restoration building stone have been obtained from laboratory tests ISRM [27] and used to determine the apparent porosity, absorption, bulk density and apparent density values of the samples. The specimens used in these standards were tested in a dry state or in water without being checked for the degree of saturation.

The aim of this test was to create controlled water saturation in stones and to examine the effects of such saturation. For this purpose, three samples of each stone unit were prepared for each experiment. The samples were dried in a 105ºC oven for 24 hours and then cooled to room temperature. Next, the water absorption ratio was determined using Eq. (6),

$$w_m = \frac{m_w - m_d}{m_d} \times 100, \tag{6}$$

where w_m is the water content, m_w refers to the water-saturated weight and m_d is the dry weight.

3 Results and discussion

3.1 Microstructural characterization

3.1.1 Petrography

The petrographic analysis was then carried out with the aim of determining the type of natural stones, their minerals, textures and geological class. Both the OBS and RBS samples exhibited microlitic porphyritic and vesicular textures and nearly the same mineralogical and textural characteristics. They had abundant plagioclase as phenocrysts and microlites (Fig. 3). Almost all phenocrystals exhibited albite twinning, and some of them also exhibited zoning The second most abundant mineral was K-feldspars as microcrystals in the mass (Fig. 3). The ferromagnesian

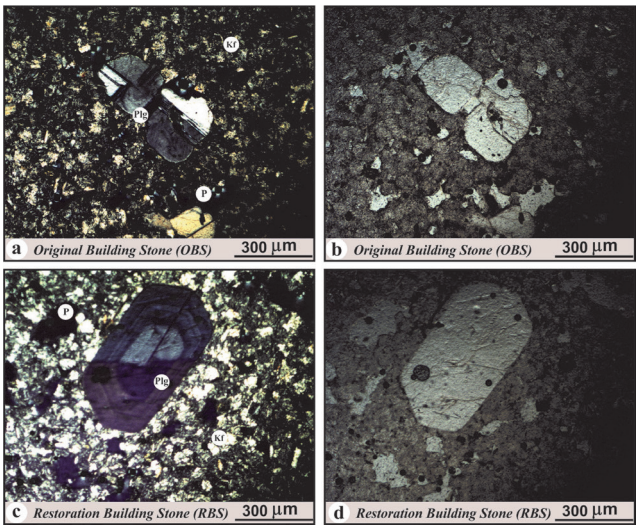

Fig. 3 Photomicrographs of the OBS and RBS (a, c: CPL: Crossed Polarised Light; b,d: PPL: Plain Polarised Light; Plg: Plagioclase, Kf: K-feldspar, P: Pore space)

mineral of both rock units was biotite with needle-shaped crystals showing pleocroism. The opaque minerals of the rocks were generally secondary opaques characterised by iron oxide minerals. Some idiomorphic primary Fe-oxide crystals were also noted in the rocks.

3.1.2 XRF

Major-trace element analyses for the original and restoration building stones are provided in Table 1. Main oxides and most significant trace elements are considered important for both stones. There has been the study on the major and trace element determination in tuff stones from Malatya. In general, the major oxides in both rocks are similar (Table 1). The original building stone and the restoration stone exhibit similarities in their geochemical characteristics. Both rock samples are plotted in the Calc-alkaline series field in the AFM diagram of Irvine and Baragar [28] (Fig. 4(a)) and the Subalkaline field in the diagram based on total alkalies ($K_2O + Na_2O$) vs silica (SiO_2) by Le Bas et al. [29] (Fig. 4(b)). Those rocks are represented by rhyolitic rocks with a typical high concentration of SiO_2 (73.8 % in OBS and 72.7 % in RBS) (Table 1, Fig. 4(b)).

3.1.3. Scanning Electron Microscopy (SEM)

SEM images of the untreated OBS and RBS samples are shown in Figs. 5(a) and 5(b), respectively. We chemically analyzed these samples using electron dispersive analysis of X-rays (EDS).

Table 1 Major and trace element contents of the OBS and RBS

Original Building Stone (OBS)	Major oxides (%)	**SiO_2**	**TiO_2**	**Al_2O_3**	**FeO***	**MnO**	**MgO**	**CaO**	**Na_2O**	**K_2O**	**P_2O_5**	**LOI**	**Cr_2O_3**	**Total**
		73.8	0.1	14.4	1.4	0.0	0.4	1.5	3.7	3.9	0.1	0.6	0.0	99.8
	Minor Elements (ppm)	**Co**	**Ni**	**Cu**	**Zn**	**Ga**	**Ge**	**As**	**Se**	**Br**	**Rb**	**Sr**	**Y**	**Zr**
		10.1	4.3	0.7	33.1	19.3	0.7	2.8	0.3	0.5	151.0	220.2	9.0	130.3
		Nb	**Mo**	**Cd**	**In**	**Sn**	**Sb**	**Te**	**I**	**Cs**	**Ba**	**La**	**Ce**	**Hf**
		9.2	2.3	0.7	0.7	2.6	0.8	1.1	2.0	3.5	637.4	34.2	67.3	4.0
		Ta	**W**	**Hg**	**Tl**	**Pb**	**Bi**	**Th**	**U**					
		1.2	145.8	1.1	0.7	26.8	0.5	23.6	6.5					
Restoration Building Stone (RBS)	Major oxides (%)	**SiO_2**	**TiO_2**	**Al_2O_3**	**FeO***	**MnO**	**MgO**	**CaO**	**Na_2O**	**K_2O**	**P_2O_5**	**LOI**	**Cr_2O_3**	**Total**
		72.7	0.1	14.2	1.4	0.0	0.5	1.8	3.6	3.9	0.1	1.3	0.0	99.7
	Minor Elements (ppm)	**Co**	**Ni**	**Cu**	**Zn**	**Ga**	**Ge**	**As**	**Se**	**Br**	**Rb**	**Sr**	**Y**	**Zr**
		13.4	3.6	0.8	34.1	19.3	0.6	3.0	0.3	0.2	149.5	215.2	9.5	126.3
		Nb	**Mo**	**Cd**	**In**	**Sn**	**Sb**	**Te**	**I**	**Cs**	**Ba**	**La**	**Ce**	**Hf**
		10.5	2.7	0.8	0.8	1.3	0.9	1.2	2.1	3.6	624.8	34.6	69.1	5.9
		Ta	**W**	**Hg**	**Tl**	**Pb**	**Bi**	**Th**	**U**					
		3.7	135.3	1.2	1.7	26.4	0.5	21.8	6.7					

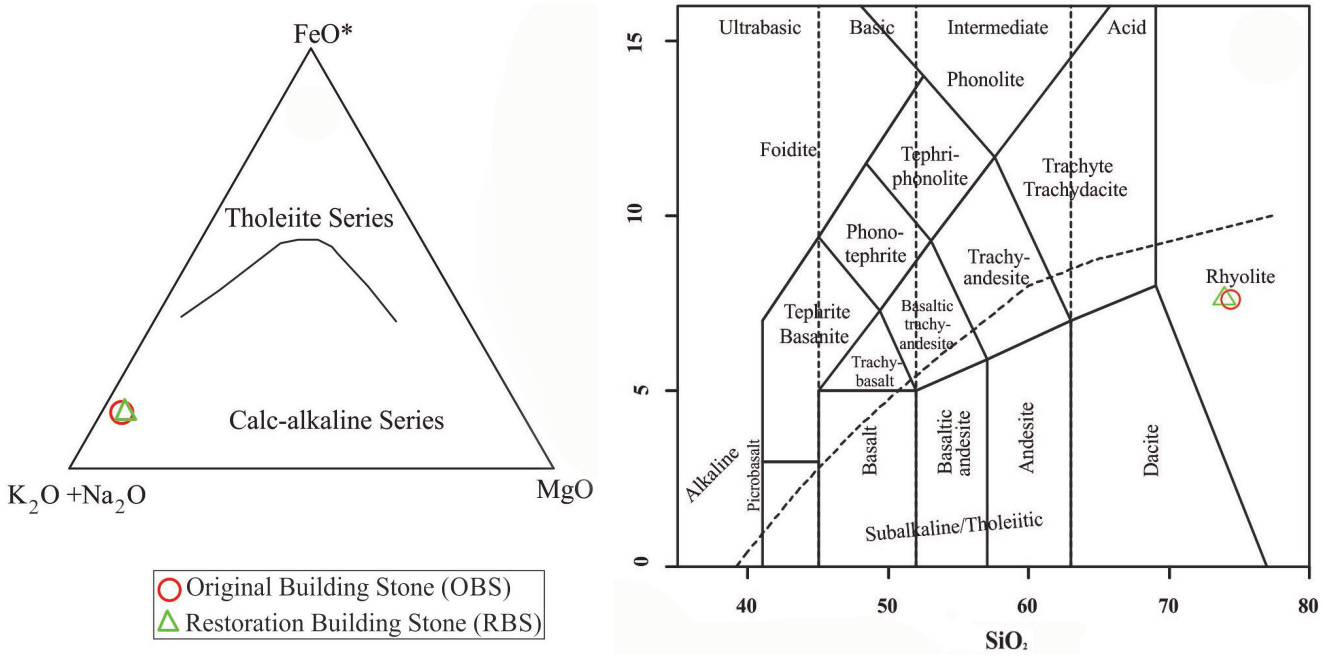

Fig. 4 a) AFM (Irvine and Baragar, [28]) and b) rock classification (Le Bas et al. [29]) diagrams for the OBS and RBS

The surface of the construction material samples exhibited small cracks in different directions. The EDS analysis of the OBS and RBS materials revealed the presence of silica and aluminium. The RBS and OBS materials were similar in terms of the results of the microstructural analyses.

3.2 Determination of the dynamic elastic modulus using NDT

Measurements were taken from five different buildings, and the dynamic elastic modulus and Poisson's ratio were determined in Table 2. In the study, the values were calculated by taking the average of three measurements from each region. The experimental data were analyzed to determine the most appropriate relationship between the dynamic elastic modulus and the P- and S-wave velocities. We found that as the P- and S-wave velocities increased the elastic modulus also increased. Similarly, according to the results published by Motra and Stutz [30], the dynamic modulus of the elasticity increases with an increase in the wave velocity. Also, in this research, the class, range and

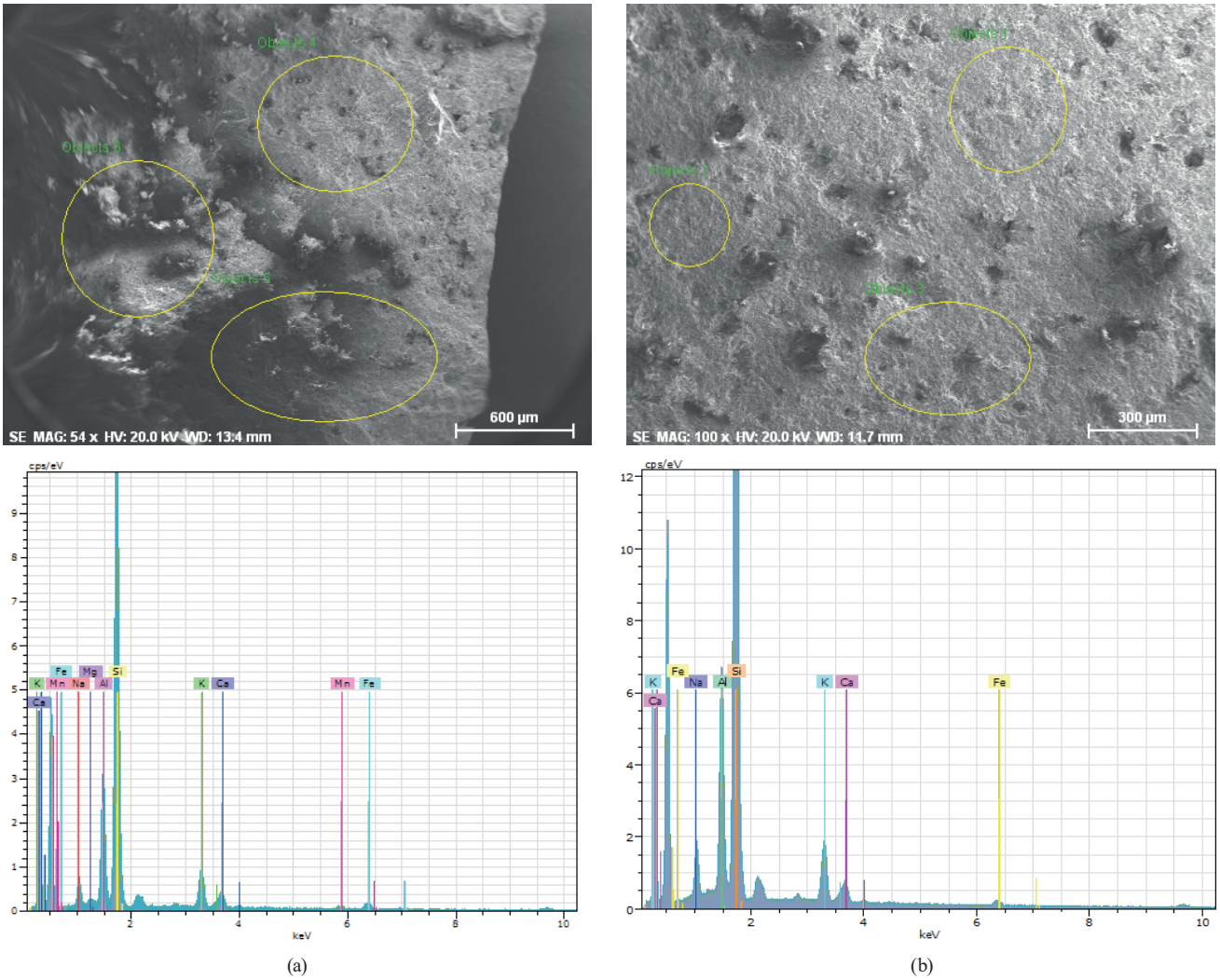

(a) (b)

Fig. 5 SEM micrographs of the studied images showing the surface of the tuff stones with EDS analysis showing peaks corresponding to the elements, a) OBS; b) RBS

Table 2 Determination of the longitudinal (P), shear (S) wave velocities and dynamic elastic modulus

Location	ρ (g/cm^3)	v	V_p (km/s)	V_s (km/s)	Edyn (GPa)
L1	1.97	0.29	3.10	1.69	14.45
L2	2.03	0.30	3.25	1.74	15.93
L3	2.02	0.28	3.03	1.68	14.51
L4	1.98	0.29	3.05	1.66	14.06
L5	2.01	0.29	3.17	1.72	15.41
Mean	**2.00**	**0.29**	**3.12**	**1.70**	**14.87**
Variance	**0.00067**	**0.00005**	**0.0082**	**0.00102**	**0.59432**

quality of the materials were determined using the surface hardness method using samples from the walls of the structure. Table 3 below demonstrates the quality of stones for respective average rebound leebs number. The rebound number of tuff stone is classified into for types: Type A - poor (<25) , Type B - moderate (25–34), Type C - normal (35–44), Type D - very good (45<), depending on the application. L1, L3 and L4 may comply with the Type B (moderate) requirement. L2 and L5 may comply with the Type C requirement or is of normal quality. In general, the rebound number increases as the strength of the stones increases [31]. The tuff stones consume lower energy with a higher rebound value in areas with high hardness [32].

Table 3 Surface hardness of the stone using the rebound hammer

Location	Rebound leeb numbers	Class	Range	Indicated quality
L1	34	B	25-34	Moderate
L2	38	C	35-44	Normal
L3	32	B	25-34	Moderate
L4	33	B	25-34	Moderate
L5	36	C	35-44	Normal

The relationship between the results of the ultrasonic velocity test and the rebound hammer test of the structural walls is shown in Fig. 6. Regression analysis indicated a reliable linear relation between the rebound hammer test and UPV, which enabled acceptable prediction of the external structure wall using the NDT method. P-wave velocities were also greater than the S-wave velocities. According to Ji et al. [33], the velocity difference between P-wave velocities and S-wave velocities under the pressure effect mainly owes to the closing of pores and microcracks in the low-pressure range.

3.3 Determination of static elastic modulus using a mechanical test

The mechanical tests were performed on specimens used in restoration for the purpose of assessing the properties of the construction materials. The static modulus of elasticity of these materials was determined using the UCS. First, small cracks occurred with the local tension in the sample under the loading system. Then, the ultimate load capacity was reached. At that point, the sample weakened and deformation was concentrated in the materials with poor structural characteristics. As a result of the test, numerous micro-cracks occurred when the load was applied. Dall'Asta et al. [34] have noted that these microcracks were tensile cracks during the uniaxial compression test. In addition, the STS test was also performed.

The acquired parameters in terms of the mechanical properties of the construction materials are indicated in Table 4. Regression analysis was conducted (Fig. 7) to evaluate the ratio of the STS to the compressive strength. Mohamad et al. [35] noted that this ratio varied between 0.10 and 0.15 for normal-strength samples; the same ratio was between 0.06 and 0.08 for a very high-strength sample. In our experimental study, the ratio of STS to compressive strength was roughly 0.15. The tensile strength of the construction material specimens, as measured by the STS test, ranged between 2.22 MPa and 1.66 MPa. Similarly, Liang et al. [36] stated that the lowest tensile strength they recorded was 1.7 MPa. As the compressive strength of material increases, so does its splitting tensile strength. Consequently, the relationship of the STS compared with the compressive strength was evaluated using linear regression analysis. We found a strong correlation between the properties.

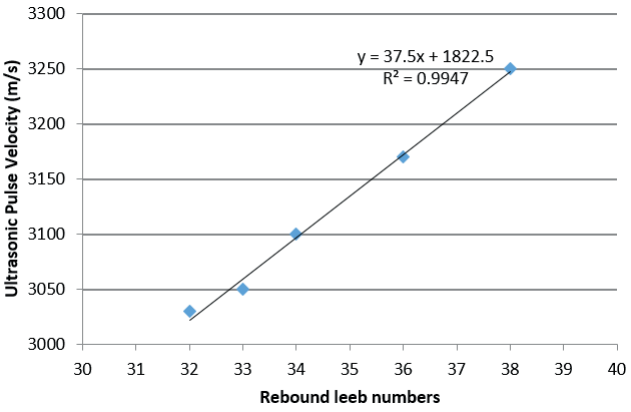

Fig. 6 Plotting of the ultrasonic velocity (V_p) versus rebound leeb numbers

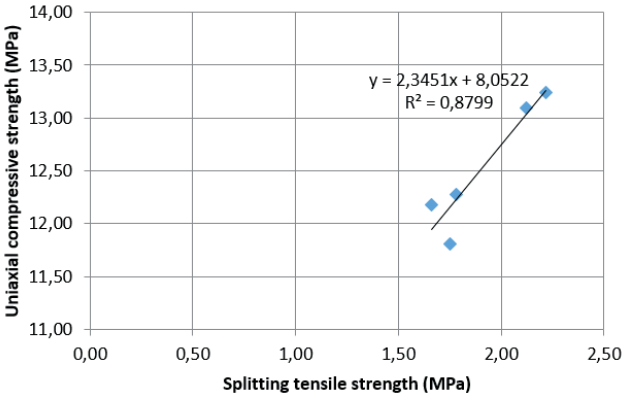

Fig. 7 Plotting of the uniaxial compressive strength (*UCS*) versus splitting tensile strength (*STS*)

Table 4 Mechanical properties of the construction materials

Sample	Poisson's ratio (ν)	E_s (GPa)	*UCS* (MPa)	*STS* (MPa)
M1	0.29	13.10	12.28	1.78
M2	0.30	13.42	13.24	2.22
M3	0.28	12.78	12.18	1.66
M4	0.29	12.27	11.81	1.75
M5	0.29	13.15	13.10	2.12
Mean	**0.29**	**12.94**	**12.52**	**1.91**
Variance	**0.00005**	**0.19363**	**0.38302**	**0.06128**

3.4 Comparison of dynamic and static modulus of elasticity of the building materials

Mechanical characteristics are largely associated with their elasticity; a higher value shows reflects a greater strength capacity with less deflection. Structural elements with the high mechanical strength have high values of dynamic and static elastic modulus. The results revealed by both methods showed that the static and dynamic elastic moduli were closely linked (Fig. 8). On the basis of statistical regression analysis, a good correlation was found (R^2 = 0.72). This finding indicates that a reliable calculation of static elastic modulus of a sample can be obtained from the dynamic elastic modulus. The dynamic Young's modulus is roughly 5–20 % higher than the static Young's modulus. Sonderegger et al. [37] stated that the difference between the dynamic and static modulus of elasticity values can be linked to the heterogeneous microstructure of the structural materials.

3.5 Physical properties of the specimens

The bulk density values of the specimens ranged from 1.82–1.92 M.g/m^3; the largest relative density was determined to be 2.03 M.g/m^3 in a moderate unit weighted sample class. The structural samples exhibited a minimum open porosity value of 12.44 %; the maximum open porosity value was found to be 15.73 %. In addition, the average open porosity value was determined to be 14.18 %, which corresponds to a medium porosity. Fig. 9 showed using a set of statistical correlations between absorption and porosity. A correlation (R^2 = 0.67) was found between water absorption and the porosity of the samples. Consequently, those specimens that exhibited lower absorption also exhibited strong mechanical properties. Similarly, Yu et al. [38] reported that the effective strength of the stone materials increased as their water-absorption capacity decreased.

4 Conclusions

Heritage masonry buildings have been exposed to many earthquakes throughout the history. Therefore, many damages occurred in these structures after earthquakes. In this study, we determined the microstructural, mechanical and physical properties of tuff blocks used for restoration in historical buildings. We found that:

- OBS and RBS samples exhibited similar chemical composition according to XRF and petrography studies.
- These samples were of volcanic origin and generally fell into the rhyolitic class according to the XRF analysis.
- Regression analysis revealed a strong correlation between the calculated and tested elastic modulus, which justified the use of NDT methods in the calculations.
- As P- and S-wave velocity increased, seismic elastic modulus also increased.
- The calculated dynamic elastic modulus (seismic modulus) was greater than the tested static elastic modulus.
- Regression analysis showed that there was a reliable linear relationship between the results of the rebound hammer test and UPV.
- The ratio of tensile strength to compressive strength was calculated to be roughly 0.15 for the samples.
- Samples with lower absorption exhibited strong mechanical properties.
- Generally, the value of the static modulus of elasticity decreased with decreasing strain ratio.

Disclosure statement

No potential conflict of interest was reported by the authors.

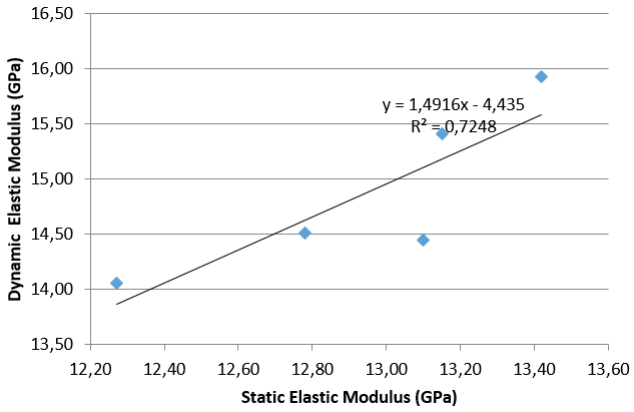

Fig. 8 Plotting of the dynamic elastic modulus (E_{dyn}) versus static elastic modulus (E_s)

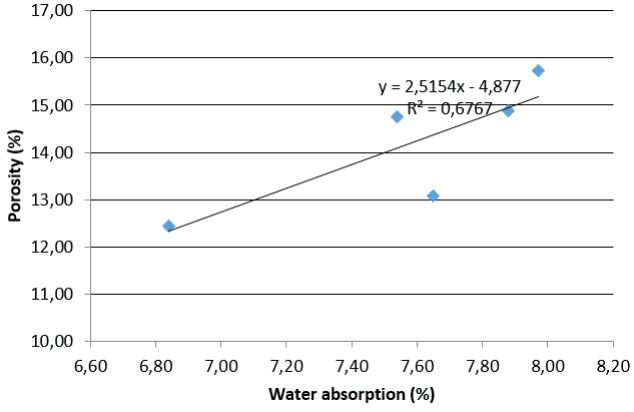

Fig. 9 Plotting of the porosity versus water absorption

Funding

The authors are grateful to the Kahramanmaras Sutcu Imam University (KSU) Project of Scientific Investigation (PSI) for their financial support for this project, (2015/1-69D) and to Prof. Dr. Yusuf Kaan Kadıoglu, (YEBIM) at Ankara University for making XRF analysis.

References

[1] Malek, J., Kaouther, M. "Destructive and Non-destructive Testing of Concrete Structures", Journal of Civil Engineering, 8(4), pp. 432–441, 2014.

[2] Binda, L., Lualdi, M., Saisi, A. "Investigation strategies for the diagnosis of historic structures: on-site tests on Avio Castle, Italy, and Pišece Castle, Slovenia", Canadian Journal Civil Engineering, 35(6), pp. 555–566, 2008. https://doi.org/10.1139/L07-143

[3] Baratta, A., Corbi, I., Corbi, O. "Bounds on the Elastic Brittle solution in bodies reinforced with FRP/FRCM composite provisions", Composite Part B: Engineering, 68, pp. 230–236, 2015. https://doi.org/10.1016/j.compositesb.2014.07.027

[4] Maras, M. M., Kose, M. M. "Structural Behavior of Masonry Panels Strengthened Using Geopolymer Composites in Compression Tests", Iranian Journal of Science and Technology, Transactions of Civil Engineering, 2020. https://doi.org/10.1007/s40996-020-00433-6

[5] Seshu, D. R., Dakshina Murthy, N. R. "Non Destructive Testing of Bridge Pier - Case Study", Procedia Engineering, 54, pp. 564–572, 2013. https://doi.org/10.1016/j.proeng.2013.03.051

[6] Binda, L., Saisi, A., Tiraboschi, C. "Investigation procedures for the diagnosis of historic masonries", Construction and Building Materials, 14(4), pp. 199–233, 2000. https://doi.org/10.1016/S0950-0618(00)00018-0

[7] Ludovico-Marques, M., Chastre, C., Vasconcelos, G. "Modelling the compressive mechanical behaviour of granite and sandstone historical building Stones", Construction and Building Materials, 28(1), pp. 372–381, 2012. https://doi.org/10.1016/j.conbuildmat.2011.08.083

[8] Török, Á., Přikryl, R. "Current methods and future trends in testing, durability analyses and provenance studies of natural stones used in historical monuments", Engineering Geology, 115(3–4), pp. 139–142, 2010. https://doi.org/10.1016/j.enggeo.2010.07.003

[9] Apostolopoulou, A. P., Carvoeiras, L. M., Klonari, A. "Cultural Heritage and education: Integrating tour maps in a Bilateral Project", European Journal of Geography, 5(4), pp. 67–77, 2014.

[10] Binda, L., Modena, C., Baronio, G., Abbaneo, S. "Repair and investigation techniques for stone masonry walls", Construction and Building Materials, 11(3), pp. 133–142, 1997. https://doi.org/10.1016/S0950-0618(97)00031-7

[11] Masciotta, M.-G., Roque, J. C. A., Ramos, L. F., Lourençco, P. B. "A multidisciplinary approach to assess the health state of heritage structures: The case study of the Church of Monastery of Jerónimos in Lisbon", Construction and Building Materials, 116, pp. 169–187, 2016. https://doi.org/10.1016/j.conbuildmat.2016.04.146

[12] Huang, X., Qi, S., Guo, S., Dong, W. "Experimental Study of Ultrasonic Waves Propagating Through a Rock Mass with a Single Joint and Multiple Parallel", Rock Mechanics and Rock Engineering, 47, pp. 549–559, 2014. https://doi.org/10.1007/s00603-013-0399-2

[13] Słota-Valim, M. "Static and dynamic elastic properties, the cause of the difference and conversion methods – case study", Nafta-Gaz, 11, pp. 816–826, 2015. https://doi.org/10.18668/NG2015.11.02

[14] Alexander, A. M., Thorton, Jr., H. T. "Ultrasonic Pitch-Catch and Pulse-Echo Measurements in Concrete", In: Lew, H. S. (ed.) ACI SP-112 Non-destructive Testing of Concrete, American Concrete Institute, Farmington Hills, MI, USA, 1989, pp. 21–40.

[15] Aggelakopoulou, E., Bakolas, A., Moropoulou, A. "Design and evaluation of concrete for restoration interventions on Byzantine monuments", Journal of Cultural Heritage, 34, pp. 166–171, 2018. https://doi.org/10.1016/j.culher.2018.05.006

[16] Lim, M. K., Cao, H. "Combining multiple NDT methods to improve testing effectiveness", Construction and Building Materials, 38, pp. 1310–1315, 2013. https://doi.org/10.1016/j.conbuildmat.2011.01.011

[17] Lubelli, B., Nijland, T. G., Tolboom, H.-J. "Moisture induced weathering of volcanic tuffstone", Construction and Building Materials, 187, pp. 1134–1146, 2018. https://doi.org/10.1016/j.conbuildmat.2018.08.002

[18] Heap, M. J., Farquharson, J. I., Kushnir, A. R. L., Lavallée, Y., Baud, P., Gilg, H. A., Reuschlé, T. "The influence of water on the strength of Neapolitan Yellow Tuff, the most widely used building stone in Naples (Italy)", Bulletin of Volcanology, 80, Article number: 51, 2018. https://doi.org/10.1007/s00445-018-1225-1

[19] Germinario, L., Török, Á. "Surface Weathering of Tuffs: Compositional and Microstructural Changes in the Building Stones of the Medieval Castles of Hungary", Minerals, 10(4), Article number: 376, 2020. https://doi.org/10.3390/min10040376

[20] Doehne, E., Simon, S., Mueller, U., Carson, D., Ormsbee, A. "Characterization of carved rhyolite tuff–The Hieroglyphic Stairway of Copán, Honduras", Restoration Building Monument, 11(4), pp. 247–254, 2005.

[21] ASTM "ASTM D 2845-05 Standard Test Method for Laboratory Determination of Pulse Velocities and Ultrasonic Elastic Constants of Rock", ASTM International, West Conshohocken, PA, USA, 2005. https://doi.org/10.1520/D2845-05

[22] ASTM "ASTM D 5873-14 Standard Test Method for Determination of Rock Hardness by Rebound Hammer Method", West Conshohocken, PA, USA, 2014. https://doi.org/10.1520/D5873-14

[23] Perras, M. A., Diederichs, M. S. "A Review of the Tensile Strength of Rock: Concepts and Testing", Geotechnical and Geological Engineering, 32, pp. 525–546, 2014.
https://doi.org/10.1007/s10706-014-9732-0

[24] ISRM "Suggested Methods for Determining the Uniaxial Compressive Strength and Deformability of Rock Materials", International Journal of Rock Mechanics and Mining Sciences, 15, pp. 99–103, 1978.
https://doi.org/10.1016/0148-9062(78)90003-7

[25] CEN "Eurocode 7 - Geotechnical design - Part 2: Ground investigation and testing", European Committee for Standardization, Brussels, Belgium, 2007.

[26] Briševac, Z., Kujundžić, T., Čajić, S. "Current Cognition of Rock Tensile Strength Testing by Brazilian Test", The Mining-Geology-Petroleum Engineering Bulletin, 30(2), 101–114, 2015.
https://doi.org/10.17794/rgn.2015.2.2

[27] ISRM "SM for determining water content, porosity, density, absorption and related properties and swelling and slake-durability index properties", ISRM Suggested Methods, 2, pp. 92–94, 1977.

[28] Irvıne, T. N., Baragar, W. R. A. "A Guide to the Chemical Classification of the Common Volcanic Rocks", Canadian Journal of Earth Sciences, 8(5), pp. 523–548, 1971.
https://doi.org/10.1139/e71-055

[29] Le Bas, M. J., Le Maitre, R. W., Streckeisen, A., Zanettin, B. "A Chemical Classification of Volcanic Rocks Based on the Total Alkali-Silica Diagram", Journal of Petrology, 27(3), pp. 745–750, 1986.
https://doi.org/10.1093/petrology/27.3.745

[30] Motra, H. B., Stutz, H. H. "Geomechanical Rock Properties Using Pressure and Temperature Dependence of Elastic P- and S-Wave Velocities", Geotechnical and Geological Engineering, 36, pp. 3751–3766, 2018.
https://doi.org/10.1007/s10706-018-0569-9

[31] Fort, R., de Buergo, M. A., Perez-Monserrat, E. M. "Non-destructive testing for the assessment of granite decay in heritage structures compared to quarry stone", International Journal of Rock Mechanics and Mining Sciences, 61, pp. 296–305, 2013.
https://doi.org/10.1016/j.ijrmms.2012.12.048

[32] Viles, H., Goudie, A., Grab, S., Lalley, J. "The use of the Schmidt Hammer and Equotip for rock hardness assessment in geomorphology and heritage science: a comparative analysis", Earth Surface Processes and Landforms, 36(3), pp. 320–333, 2011.
https://doi.org/10.1002/esp.2040

[33] Ji, S., Li, L., Motra, H. B., Wuttke, F., Sun, S., Michibayashi, K., Salisbury, M. H. "Poisson's ratio and Auxetic Properties of Natural Rocks", JGR Solid Earth, 123(2), pp. 1161–1185, 2018.
https://doi.org/10.1002/2017JB014606

[34] Dall'Asta, A., Leoni, G., Meschini, A., Petrucci, E., Zona, A. "Integrated approach for seismic vulnerability analysis of historic massive defensive structures", Journal of Cultural Heritage, 35, pp. 86–98, 2019.
https://doi.org/10.1016/j.culher.2018.07.004

[35] Mohamad, E. T., Armaghani, D. J., Momeni, E., Alavi, S. V., Abad, S. V. A. N. K. "Prediction of the unconfined compressive strength of soft rocks: a PSO-based ANN approach", Bulletin of Engineering Geology and the Environment, 74, pp. 745–757, 2015.
https://doi.org/10.1007/s10064-014-0638-0

[36] Liang, M., Mohamad, E. T., Khun, M. C., Alel, M. N. A. "Estimating Uniaxial Compressive Strength of Tropically Weathered Sedimentary Rock Using Indirect", Jurnal Teknologi, 72(3), pp. 49–58, 2015.
https://doi.org/10.11113/jt.v72.4013

[37] Sonderegger, W., Kránitz, K., Bues, C.- T., Niemz, P. "Aging effects on physical and mechanical properties of spruce, fir and oak wood Walter", Journal of Cultural Heritage, 16(6), pp. 883–889, 2015.
https://doi.org/10.1016/j.culher.2015.02.002

[38] Yu, C., Ji, S., Li, Q. "Effects of porosity on seismic velocities, elastic moduli and Poisson's ratios of solid materials and rocks", Journal of Rock Mechanics and Geotechnical Engineering, 8(1), pp. 35–49, 2016.
https://doi.org/10.1016/j.jrmge.2015.07.004